# Handheld array-based photoacoustic probe for guiding needle biopsy of sentinel lymph nodes

**Chulhong Kim**
Washington University in St. Louis
Department of Biomedical Engineering
Optical Imaging Laboratory
Campus Box 1097, One Brookings Drive
St. Louis, Missouri 63130-4899

**Todd N. Erpelding**
Philips Research North America
345 Scarborough Road
Briarcliff Manor, New York 10510

**Konstantin Maslov**
Washington University in St. Louis
Department of Biomedical Engineering
Optical Imaging Laboratory
Campus Box 1097, One Brookings Drive
St. Louis, Missouri 63130-4899

**Ladislav Jankovic**
Philips Research North America
345 Scarborough Road
Briarcliff Manor, New York 10510

**Walter J. Akers**
Washington University School of Medicine
Department of Radiology
and
Department of Biophysics
Optical Radiology Laboratory
4525 Scott Avenue
Saint Louis, Missouri 63108

**Liang Song**
Washington University in St. Louis
Department of Biomedical Engineering
Optical Imaging Laboratory
Campus Box 1097, One Brookings Drive
St. Louis, Missouri 63130-4899

**Samuel Achilefu**
Washington University School of Medicine
Department of Radiology
and
Department of Biophysics
Optical Radiology Laboratory
4525 Scott Avenue
Saint Louis, Missouri 63108

**Julie A. Margenthaler**
Washington University School of Medicine
Department of Surgery
Campus Box 8109, 660 South Euclid Avenue
St. Louis, Missouri 63110

**Michael D. Pashley**
Philips Research North America
345 Scarborough Road
Briarcliff Manor, New York 10510

**Lihong V. Wang**
Washington University in St. Louis
Department of Biomedical Engineering
Optical Imaging Laboratory
Campus Box 1097, One Brookings Drive
St. Louis, Missouri 63130-4899

**Abstract.** By modifying a clinical ultrasound array system, we develop a novel handheld photoacoustic probe for image-guided needle biopsy. The integration of optical fiber bundles for pulsed laser light delivery enables photoacoustic image-guided insertion of a needle into rat axillary lymph nodes with accumulated indocyanine green (ICG). Strong photoacoustic contrast of the needle is achieved. After subcutaneous injection of the dye in the left forepaw, sentinel lymph nodes are easily detected, *in vivo* and in real time, beneath 2-cm-thick chicken breast overlaying the axillary region. ICG uptake in axillary lymph nodes is confirmed with fluorescence imaging both *in vivo* and *ex vivo*. These results demonstrate the clinical potential of this handheld photoacoustic system for facile identification and needle biopsy of sentinel lymph nodes for cancer staging and metastasis detection in humans.  [DOI: 10.1117/1.3469829]

Keywords: image-guided needle biopsy; photoacoustic imaging; ultrasound array system; sentinel lymph node biopsy.

Paper 10162R received Mar. 26, 2010; revised manuscript received May 25, 2010; accepted for publication May 28, 2010; published online Aug. 16, 2010.

## 1 Introduction

Sentinel lymph node (SLN) biopsy has become the standard of care for patients diagnosed with breast cancer, replacing axillary lymph node dissection. Biopsy of the lymph nodes directly draining the tumor area can accurately stage cancer to guide therapeutic decisions. Ultrasound (US) guidance of minimally invasive interventions is widely performed, leading to improved treatment outcomes and shorter recovery.[1,2] Real-time, noninvasive, nonionizing, and portable US imaging is currently the primary method for guiding targeted needle biopsies and nerve blockings.[3,4]

Photoacoustic (PA) imaging is a nonionizing and noninvasive hybrid imaging technique that combines strong optical absorption contrast with high ultrasonic spatial resolution.[5] Since ultrasonic scattering is 2 to 3 orders of magnitude less than optical scattering, PA imaging can break through the fundamental depth limitations of pure optical imaging.[6] Using

Address all correspondence to: Lihong V. Wang, Optical Imaging Laboratory, Department of Biomedical Engineering, Washington University in St. Louis, Campus Box 1097, One Brookings Drive, St. Louis, MO 63130-4899. Tel: 314-935-6152; Fax: 314-935-7448; E-mail: lhwang@biomed.wustl.edu

1083-3668/2010/15(4)/046010/4/$25.00 © 2010 SPIE

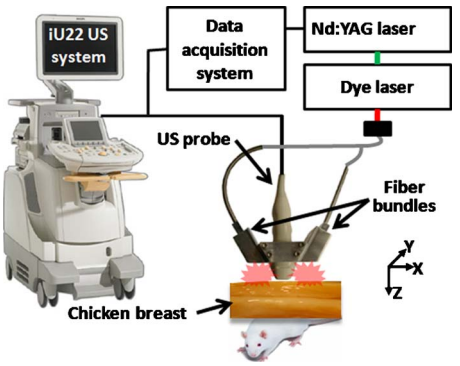


**Fig. 1** Schematic of the integrated PA and US imaging system based on a clinical ultrasound scanner (iU22, Philips Healthcare).

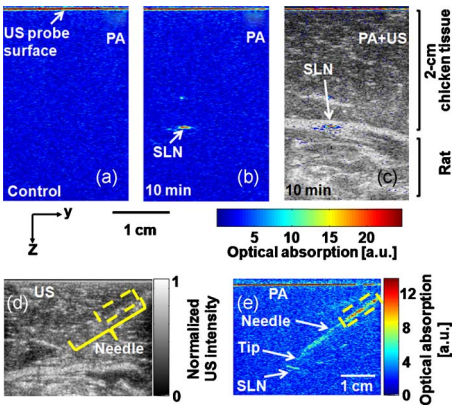


**Fig. 2** *In vivo* PA and US B-scan imaging of an SLN dyed with ICG and guiding of a biopsy needle: (a) control PA image acquired before ICG injection, (b) PA image taken 10 min after ICG injection, (c) overlaid PA (pseudocolor) and US (gray scale) images, (d) US guidance of a biopsy needle, and (e) PA guidance of a biopsy needle. The image contrasts were calculated using the values within the regions of interest indicated by the yellow dotted boxes in (d) and (e). PA, photoacoustic; US, ultrasound; ICG, indocyanine green; and SLN, sentinel lymph node. (Color online only.)

intrinsic contrasts such as hemoglobin or melanin, PA imaging can provide both morphological and functional information.[5] Moreover, using molecularly targeted exogenous contrast agents, it can also provide molecular information.[5] We previously reported *in vivo* detection of lymph nodes in rats using a raster-scanning tabletop PA imaging system. Methylene blue,[7] indocyanine green (ICG),[8] and gold nanoparticles[9] were used as contrast agents. However, this system was relatively slow for clinical applications (20 min for a 20-$\times$20-mm$^2$ field of view), and its imaging head was not handheld. We also reported *in vivo* PA and US mapping of SLNs in rats using a US array, but the light delivery was not handheld.[10]

In this paper, for the first time to our knowledge, we report noninvasive *in vivo* mapping of deeply positioned ICG-dyed SLNs ($\sim$2.1 cm) in rats using a PA imaging system adapted from a commercial US array system. A US probe integrated with optical fiber bundles for light delivery enabled handheld scanning as in ultrasonography.[11,12] ICG uptake in SLNs was confirmed by fluorescence imaging. Furthermore, both real-time PA imaging [1 frame per second (fps)] and US imaging (5 fps) successfully guided needle insertion *in vivo*.

## 2 Methods and Materials

Figure 1 shows an experimental schematic of the integrated PA and US imaging system, adapted from a clinical US imaging system[10] (iU22, Philips Healthcare). Raw per-channel PA and US data were both acquired through the modified channel board architecture and transferred to a custom-made data acquisition computer for display and postprocessing. The data acquisition system was synchronized with laser firing. Fourier-beam-formed PA images were displayed at a frame rate of $\sim$1 fps. However, the frame rate can be improved to 10 fps, limited by the current laser repetition rate. US images were captured at 5 fps. For this study, we used a linear array US probe (L8-4, Philips Healthcare) with a nominal bandwidth of 4 to 8 MHz. Light from a tunable dye laser (NS, Sirah), pumped by a *Q*-switched Nd:YAG laser (PRO-350-10, Newport) with a 6.5-ns pulse duration and a 10-Hz pulse repetition rate, was coupled to a multimode fiber bundle (CB18043, Fiberguide). The fiber bundle was bifurcated and physically integrated with the US probe, enabling handheld scanning. The two optical beams were obliquely incident ($\sim$45 deg) on the tissue surface as rectangles (2$\times$3 cm along the *X* and *Y* axes from each bundle). An optical wavelength of 810 nm, close to the peak optical absorption wavelength of ICG (806 nm in albumin), was utilized. Light fluence on the skin was less than 1.5 mJ/cm$^2$, well below the American National Standards Institute safety limits.[13] Tabletop PA imaging systems and the previously reported study using this modified Philips system required a water tank, which is clinically undesirable. Here, US gel was applied to directly couple the PA probe to the surface of the tissue.

Animal handling was performed according to the guidelines on the care and use of laboratory animals at Washington University in St. Louis. Sprague Dawley rats ($\sim$200 g) were initially anesthetized using a mixture of ketamine (85 mg/kg) and xylazine (15 mg/kg). To test the clinical feasibility of this technique on humans, we intentionally increased the imaging depth by laying $\sim$2 cm of chicken tissue atop the rat. After depilation in the left axillary region, we first obtained a control PA image before the injection of ICG. After intradermally injecting 0.1 ml of 1-mM ICG into the left forepaw, we acquired a series of PA images to monitor the ICG uptake in the SLN dynamically. Then, we demonstrated PA image-guided needle (18 gauge) insertion *in vivo*. Here, we mechanically fixed the PA imaging probe to avoid motion artifacts. After PA imaging, *in vivo* fluorescence imaging was performed with a time-domain diffuse optical imaging system (eXplore Optix, Advance Research Technologies) to confirm ICG uptake. Then, *ex vivo* fluorescence imaging was performed to confirm uptake in the lymph nodes using a planar reflectance imaging system (Kodak IS4000MM, Carestream Health) with 755-nm excitation and 830-nm detection.

## 3 Results and Discussion

To investigate the feasibility of PA and US mapping of SLNs with ICG, we imaged the left axillary region in a rat before and after ICG injection. A control PA B-scan image was acquired before injection [Fig. 2(a)]. Immediately after injec-

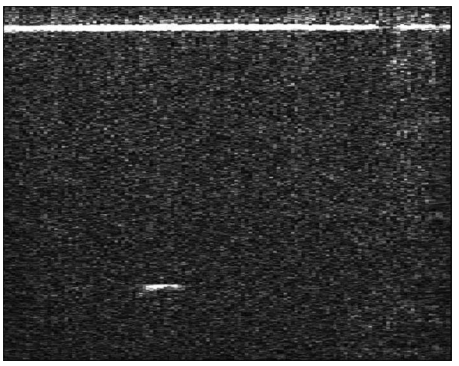

**Video 1** Dynamic PA imaging of ICG accumulation in the SLN *in vivo* (QuickTime, 7.4 MB). [URL: http://dx.doi.org/10.1117/1.3469829.1].

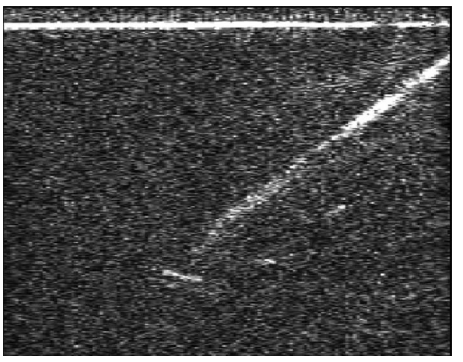

**Video 3** PA guidance of a biopsy needle (QuickTime, 6.6 MB). [URL: http://dx.doi.org/10.1117/1.3469829.3].

tion, ICG accumulation in the deeply positioned SLN was observed photoacoustically. Video 1 shows the dynamic accumulation of ICG in the SLN. The PA image of the ICG-dyed SLN acquired at 10 min postinjection [Fig. 2(b)] shows that ICG accumulation enhanced the PA signal in the SLN by $9.5 \pm 2.7$ (standard deviation). Figure 2(c), created by overlaying the PA and US images, shows both morphological information and functional information (ICG uptake in the SLN). For comparison, the PA images in Figs. 2(a)–2(c) are displayed in the same dynamic range. A snapshot of the US-guided needle insertion is shown in Fig. 2(d). As the needle was inserted into the chicken tissue *in vivo*, it was ultrasonically tracked in real time (Video 2), but the SLN was not detected ultrasonically. The needle progression could also be detected photoacoustically, as shown in Fig. 2(e) and Video 3. PA imaging was able to detect the SLN clearly. Comparison of the two videos clearly shows that PA imaging has much higher contrast than US imaging in needle tracking under the current experimental condition. We quantified the image contrasts of the needles in both images within the regions of interest indicated by the yellow dotted boxes in Figs. 2(d) and 2(e). The PA image contrast of the needle was $8.5 \pm 4$ (standard deviation), whereas the US image contrast was $1.2 \pm 0.04$ (standard deviation). However, in neither case was the tracking of the needle optimized and both imaging modalities were highly operator-dependant.

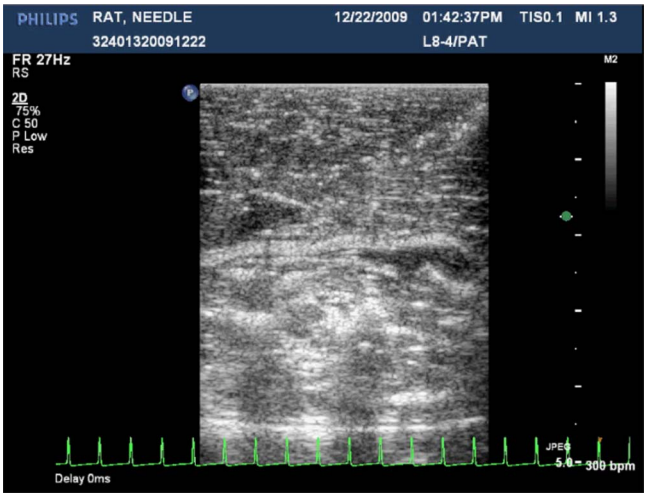


**Video 2** US guidance of a biopsy needle (QuickTime, 6.9 MB). [URL: http://dx.doi.org/10.1117/1.3469829.2].

Fluorescence images obtained after PA imaging confirmed ICG uptake in the SLN [Fig. 3(a)]. Further, we imaged fluorescently three dissected lymph nodes (LNs) from the left axillary region [Fig. 3(b)]. Only the first draining node, the sentinel node, generated strong fluorescence.

## 4 Conclusions

We developed a noninvasive, nonionizing, real-time, and handheld PA and US imaging system using a modified clinical US imaging system. *In vivo* mapping of rat SLNs at an imaging depth of ~2.1 cm was successfully accomplished following ICG injection. Further, PA imaging enabled guided needle insertion with strong contrast *in vivo*. This technique is highly translatable to clinical applications for image-guided SLN biopsy, nerve blockings, and many others.

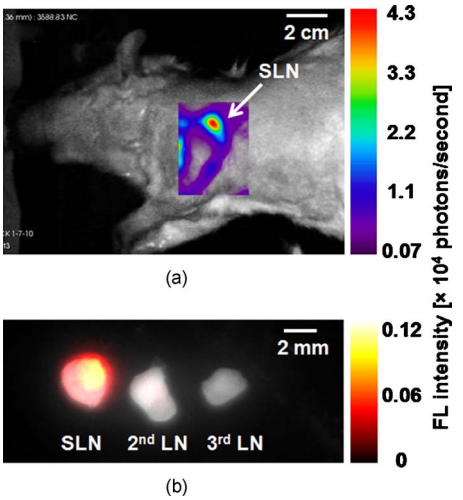


**Fig. 3** Fluorescence imaging of an SLN dyed with ICG: (a) fluorescence image of the left axillary region showing high intensity from the SLN and lymph vessels, acquired noninvasively ~1 h after injection of ICG and (b) *ex vivo* fluorescence image of LNs dissected from the same axillary region after *in vivo* imaging. Grayscale represents white light intensity, and pseudocolor represents fluorescence intensity. SLN, sentinel lymph node; ICG, indocyanine green; LN, lymph node; and FL, fluorescence.

## Acknowledgments

This work was supported in part by grants from the National Institutes of Health (Grants R01 EB000712, R01 EB008085, and U54 CA136398—the Network for Translational Research). L.V.W. has a financial interest in Microphotoacoustics, Inc., and in Endra, Inc., which, however, did not support this work. T.N.E, L.J., and M.D.P are employees of Philips Research.

## References

1. F. Laurent, V. Latrabe, B. Vergier, M. Montaudon, J. M. Vernejoux, and J. Doubrez, "CT-guided transthoracic needle biopsy of pulmonary nodules smaller than 20 mm: results with an automated 20-gauge coaxial cutting needle," *Clin. Radiol.* **55**(4), 281–287 (2000).
2. F. K. Wacker, S. Vogt, A. Khamene, J. A. Jesberger, S. G. Nour, D. R. Elgort, F. Sauer, J. L. Duerk, and J. S. Lewin, "An augmented reality system for MR image-guided needle biopsy: initial results in a swine model," *Radiology* **238**(2), 497–504 (2006).
3. B. D. Fornage, M. J. Faroux, and A. Simatos, "Breast masses: US-guided fine-needle aspiration biopsy," *Radiology* **162**, 409–414 (1987).
4. R. Knobloch, J. Weber, Z. Varga, H. Feiber, A. Heidenreich, and R. Hofmann, "Bilateral fine-needle administered local anaesthetic nerve block for pain control during TRUS-guided multi-core prostate biopsy: a prospective randomised trial," *Eur. Urol.* **41**(5), 508–514 (2002).
5. C. Kim, C. Favazza, and L. V. Wang, "In vivo photoacoustic tomography of chemicals: high-resolution functional and molecular optical imaging at new depths," *Chem. Rev.* **110**(5), 2756–2782 (2010).
6. B. W. Zeff, B. R. White, H. Dehghani, B. L. Schlaggar, and J. P. Culver, "Retinotopic mapping of adult human visual cortex with high-density diffuse optical tomography," *Proc. Natl. Acad. Sci. U.S.A.* **104**(29), 12169–12174 (2007).
7. K. H. Song, E. W. Stein, J. A. Margenthaler, and L. V. Wang, "Noninvasive photoacoustic identification of sentinel lymph nodes containing methylene blue in vivo in a rat model," *J. Biomed. Opt.* **13**(5), 054033 (2008).
8. C. Kim, K. H. Song, F. Gao, and L. V. Wang, "Noninvasive dual-modality in vivo mapping by using indocyanine green in rats—volumetric spectroscopic photoacoustic imaging and planar fluorescence imaging," *Radiology* **255**, 442–450 (2010).
9. K. H. Song, C. Kim, C. M. Cobley, Y. Xia, and L. V. Wang, "Near-infrared gold nanocages as a new class of tracers for photoacoustic sentinel lymph node mapping on a rat model," *Nano Lett.* **9**(1), 183–188 (2009).
10. T. N. Erpelding, C. Kim, M. Pramanik, L. Jankovic, K. Maslov, Z. Guo, J. A. Margenthaler, M. D. Pashley, and L. V. Wang, "Sentinel lymph nodes in the rat: Noninvasive photoacoustic and US imaging with a clinical US system," *Radiology* **256**, 102–110 (2010).
11. S. Y. Emelianov, S. R. Aglyamov, J. Shah, S. Sethuraman, W. G. Scott, R. Schmitt, M. Motamedia, A. Karpiouk, and A. A. Oraevsky, "Combined ultrasound, optoacoustic and elasticity imaging," *Proc. SPIE* **5320**, 101–112 (2004).
12. M. P. Fronheiser, S. A. Ermilov, H. P. Brecht, A. Conjusteau, R. Su, K. Mehta, and A. A. Oraevsky, "Real-time optoacoustic monitoring and three-dimensional mapping of a human arm vasculature," *J. Biomed. Opt.* **15**(2), 021305 (2010).
13. American National Standard for the Safe Use of Lasers, Standard Z136.1-2000, ANSI. Inc, New York (2002).